PROCEEDINGS, Fourteenth Workshop on Geothermal Reservoir Engineering
Stanford University, Stanford, California, January 24-26, 1989
SGP-TR-122

A CONCEPTUAL AND MATHEMATICAL MODEL OF THE LARDERELLO PRODUCTION HISTORY

GIUSEPPE NERI

ENEL U.N.G. PISA ITALY

ABSTRACT

The Larderello production history has been interpreted by the author(1987) as the consequence of an initial depletion-type production regime followed by a diffusive type one. At the moment a diffusive flow is developing vertically all over the northern part of the field. This paper presents a mathematical model of the Larderello production history which incorporates the above mentioned concepts. Such a model has been validated calculating the measured reservoir pressure drop caused by the actual production history.

1. INTRODUCTION

In a previous paper (Neri, 1987), the Larderello production history has been interpreted by the author as the consequence of an initial depletion-type production regime followed by a diffusive-type one. At the moment a diffusive flow is developing vertically all over the northern part of the field, as is shown by the wells shut-in tests described in Ref. 1. The depletion regime could have been caused by the uniform boiling of liquid water (White et al.,1971) stored in the uppermost part of the reservoir where a carbonatic formation is present. The diffusion regime starts when the boiling process becomes dominated by a boiling front which propagates down the reservoir giving origin to a process of pressure diffusion. With such a concept in mind,the reservoir can be therefore conceived as made by two different regions as illustrated in Fig.1. Region 1 represents the volume corresponding to the top of the reservoir where evaporation develops uniformly before spreading to the underlying Region 2.

2. THE MATHEMATICAL MODEL

In order to treat in mathematical terms the conceptual reservoir model, it has seemed useful to start out with a few simplifying hypotheses, to make easier the mathematical treatment of the problem.

Hypotheses:

a) All processes occurring within the reservoir are more or less isothermal.
b) The pressure gradient is negligible in Region 1 of Fig. 1, whereas in Region 2 it is small enough to allow the use of the diffusion equation to describe the pressure field.
c) Rock porosity and volumetric saturation of liquid water are homogeneous,rock permeability is homogeneous and isotropic throughout the reservoir.

With these hypotheses,and in reference to the scheme of Fig. 1,the pressure field within the reservoir can be described by the following equations:

$$(1)\quad C^* \frac{dP_1(t)}{dt} = Q_{21} - Q \qquad \text{Region 1}$$

$$(2)\quad (\text{Grad}^*\ \text{Grad})P_2(x,t) = (1/n)\ \delta P_2(x,t)/\delta t \qquad \text{Region 2}$$

where $C = c * V * \Phi$

$$Q_{21} = (K/\mu) * A * (\delta P_2/\delta x)_{x=0}$$

The initial and the boundary conditions under which equations 1 and 2 must be resolved are:

$$P_1\ (t>o) = P_2\ (x = o, t>o)$$
$$Q\ (t \geq o) \quad \text{Constant}$$

It is convenient to introduce the following dimensionless variables into equations 1 and 2;

$$C_D = \frac{C}{\Phi c A \sqrt{A}}$$

$$t_D = \frac{n}{A} t$$

$$P_{1.2.D} = \frac{K\sqrt{A}}{Q\mu} (P_{i.1.2} - P_{1.2})$$

$$x_D = \frac{x}{\sqrt{A}}$$

$P_{i,\ 1.2}$ = Initial pressure in regions 1 or 2.

P_1 depends on time only, whilst P_2 depends on depth too.

Equations 1 and 2 therefore assume the following form:

$$(1)' \quad C_D \frac{dP_{1D}}{dt_D} - \left.\frac{dP_{2D}}{d x_d}\right|_{x_d=0} = 1$$

$$(2)' (\text{Grad} * \text{Grad}) P_{2D} = \frac{dP_{2D}}{dt_D}$$

The resolution of equations (1)' and (2)' in consequence of hypothesis b), which gives us

$$P_{1D} = P_{2D} (x_D = o),\ t \geq o$$

is analogous to that of a problem of heat conduction in a semiinfinite medium whose surface is in contact with a well stirred fluid supplied with a constant amount of heat per unit of time .

H. S. Carslaw and J. C. Jaeger report (Ref. 2) a solution to this problem which, adapted to our case, acquires the form:

(3)

$$P_D (t_D,\ C_D,\ x_D = o) = 2 \sqrt{(t_D/\pi)} + C_D [e^{t_D/C_D^2} * \text{erfc}(\sqrt{t_D}/C_D) -1]$$

Such a solution is valid for a constant Q and hypothesizing that for

$X_D = 0$, then $P_{1D} = P_{2D} = P_D$ for $t_D > 0$

In eq. (3) appears the parameter C_D, which is an index of the storage capacity of region 1 of the reservoir.

The greater C_D is, longer the depletion production regime will last.

The parameter C_D, may not appear explicitly in the solution of P_D if we define an dimensionless time t_D^* given by

$$t_D^* = t_D/C_D^2$$

and at the same time define a dimensionless pressure P_D^* as

$$P_D^* = \frac{P_D}{C_D} = \frac{KA^2}{V} * \frac{(P_i^2 - P^2)}{Q\mu}$$

With these new definitions, solution (3) can be written as

$$(4) \quad P_D^* (t_D^*,\ x_D = 0) = 2\sqrt{(t_D^*/\pi)} + e^{t_D^*} * \text{erfc}(\sqrt{t_D^*}) - 1$$

Solution (4) is represented in Fig. 2 in the form of a bilogarithmic graph of P_D^* as a function of t_D^*.

From Fig. 4 it can be noted that for "small" t_D^* values, P_D^* is proportional to t_D^*, whereas for "large" t_D^*, P_D^* is proportional to $\sqrt{t_D^*}$. This is indicating that the pressure is initially controlled by the reservoir storage,then by a diffusion equation for linear flow.

3. THE RESERVOIR PRESSURE DROP AS CALCULATED WITH THE MATHEMATICAL MODEL

The solution P_D^* given by (4) constitutes an dimensionless influence function for $X_D = 0$, that is at the top of the reservoir.

If we wish to calculate the pressure drop at the top of the Larderello reservoir, we must solve the system of equations 1 and 2 in the case of variable flow Q, as the flow produced by the field has been variable over time.

Using π_D $(t_D^*,\ X_D=0)$ to indicate the solution of equations 1 and 2 in the case of variable Q over time, we will get

$$(5) \quad \pi_D(t_D^*, X_D = 0) = \int_0^{t_D} Q(\tau_D)(dP_D^*(t-\tau)_D/dt_D)d\tau_D$$

The integral (5) can be approximated as a finite sum of terms subdividing the time-span t_D into n intervals within each of which flow Q can be assumed to be constant.

With this approximation, (5) becomes

$$(6) \quad \pi_D(t_{Dn}^*, X_D=0) = \sum_{j=1}^{n} P_D^* (t_n - t_{j-1})_D (Q_j - Q_{j-1}) / Q_1$$

with $Q_o = 0$ for $t_o = 0$

In the place of the volumetric flow Q, the mass flow G can be introduced into (6), and at the same time we can define the dimensionless pressure π_D as:

$$\pi_D = \frac{K[P_1^2 - P^2]A^2}{2G_1 R^- Tz\mu V}$$

In the calculation of π_D using (6), flow G actually produced in Larderello north area (Valle Secolo) was approximated with the formula

(7) $G = G_\infty + (G_o - G_\infty)\exp(-t/\tau)$
$G_o = 1981$ t/h
$G_\infty = 625$ t/h
$\tau = 97$ months

which interpolates the measurements taken since August 1956 . The flow G, in the j-th time-period, was calculated as an arithmetical average of the G readings given by (7) at the extreme ends of the period.

In order to use eq. (7) for calculating π_D given by (6), it was necessary to match the physical time t with the dimensionless time t_D. To this purpose various values of the parameter $\bar{N} = \eta A^2/V^2$, which relates t_D to t by the relation $t_D = \bar{N}t$, have been used and a family of curves of π_D as a function of time t has been generated. These curves are represented in Fig.3

Using the pressure readings of the shut-in well No. 111, which is peripheral to the group of wells drilled in the Valle Secolo area and can be considered a monitoring well of the reservoir-top pressure, we find that the theoretical curve with $\bar{N} = 10^{-9}$ s^{-1} interpolates the experimental data of the first 200 months of production, (cf Fig. 4 where the time-scale starts in August 1956), whereas the curve with $\bar{N} = 10^{-8}$ s^{-1} interpolates better the experimental data after the 50th month from start-up of production (Fig. 5).

The interpolation is acceptable with both values of the parameter $\bar{N}$, but not outside this range.

Unfortunately well No. 111 is the only well which has been closed for some thirty years and which has shown interference with the producing wells during the field production period.

For shorter time-periods other records exist for shut-in wells which may be indicative of the reservoir's pressure.

These are the pressure-readings for wells 159, Gabbro 4, Gabbro 8, S. Dalmazio 2 and S. Dalmazio 4.

The readings for well 159, which is also located in the Valle Secolo area, follow the trend of the well 111 readings, whereas those of the wells in the Gabbro area (Gabbro 4 and Gabbro 8, S. Dalmazio 2 and 4) have a trend which seems to be that of well No.111 but delayed by some ten years, i. e.the time-lapse which separated the exploiting of the two areas. (Fig. 6)

Graphing the pressure drop of the wells belonging to the Gabbro area in bilogarithmic paper as in the Fig. 7 and 8, it may be observed that the graphs show a trend qualitatively similar to the one calculated with the mathematical model in the case of production at constant flow. Thus the physical assumptions of the mathematical model seem to hold for the various producing area of the Larderello reservoir.

4. ESTIMATES OF DIFFUSIVITY, COMPRESSIBILITY AND PERMEABILITY

By interpolating the pressure reading from well No.111 with the set of theoretical curves, we get two possible values for the following groups of parameters:

i $P_D/C_D = 0.4$; $\delta(P^2) = 100$ (bar²);
$\bar{N} = 10^{-8}$ s^{-1}

ii $P_D/C_D = 0.07$; $\delta(P^2) = 100$ (bar²);
$\bar{N} = 10^{-9}$ s^{-1}

depending on whether the interpolation is done with one or the other value for $\bar{N}$.

From the definition of P_D/C_D and putting:

$G_1 = 2000$ t/h ≈ 550 Kg/s
$R^- = 460$ J/ (Kg * °K)
$T = 500$°K
$z = 1$
$\mu = 2 \cdot 10^{-5}$ P_a * s

we get $K(A^2/V) = (200 - 1000) \cdot 10^{-12}$ m^3

Writing $V = A \cdot h$ and assuming :
A = 5 Km², the surface area occupied by wells
h = 500 m , the thickness of region 1 of the reservoir

It follows $(20 \leq K \leq 100) \cdot 10^{-3}$ Darcy

From the definitions of $\bar{N}$ we get

$$.25 \cdot 10^{-3} \leq \eta \leq 2.5 \cdot 10^{-3} \ m^2/s$$

Finally, dividing P_D/C_D by Ñ we can get the total compressibility ΦcV which depends weakly on the parameters of the fit, because, being $\delta(P^2)$ the same for both the groups of parameters, the value of ΦVc depends only on the ratio between P_D/C_D and Ñ which is $0.4*10^8$ s or $0.7*10^8$ s. Adopting the previous assumed values for A and h, we can get Φc from ΦcV. It results:

$$2*10^{-6} < \Phi c \leq 4*10^{-6} \; P_a^{-1}$$

These values for Φc are strongly affected by the assumed values of A and h. The uncertainty of V is mostly due to the doubts on h, as the surface area of the reservoir, drained by the wells, is known.

The height h should correspond to the thickness of the upper formation of the reservoir, the one known as the anhydritic formation, which does not have a homogeneous thickness, yet is around a few hundred metres. The estimated value for Φc should therefore be in the proper order of magnitude and is, according to Grant et al. (1982), typical of a two phase fluid.

5. PRESSURE DISTRIBUTION ALONG THE RESERVOIR VERTICAL AXIS

The proposed model has been so far used to fit the pressure drop, measured at reservoir top, caused by some 30 years of production. The fit allowed the evaluation of the parameter Ñ which is proportional to the diffusivity η. It now becomes possible to calculate by the model equations the pressure distribution at various reservoir depths caused by the past field exploitation.

The solution of equations 1' and 2' has been still derived by Carslaw and Jaeger. Posing P_D instead of P_D/C_D and introducing the dimensionless depth $X_D^* = X_D/C_D$, the following equation holds:

$$(8)\quad \frac{P_D}{C_D}(t_D^*, X_D^*) = 2\sqrt{\left(\frac{t_D^*}{\pi}\right)}\exp(-X_D^{*2}/4t_D^*) - (1+X_D^*)\,\mathrm{erfc}(X_D^*/2\sqrt{t_D^*}) + \exp(X_D^* + t_D^*) * \mathrm{erfc}\,[X_D/2\sqrt{t_D^*} + \sqrt{t_D^*}]$$

$$X_D = X/\sqrt{A}$$

$$X_D^* = X_D/C_D = X * A/V$$

$$t_D^* = t_D/C_D^2 = \eta * (A^2/V^2) * t$$

The dimensionless depth X_D^* is the ratio between real depth, measured from the plane separating regions 1 and 2 in the reservoir, and the thickness of region 1.

Having estimated that the parameter Ñ is within the range 10^{-9} and 10^{-8} sec^{-1}, the same method of approach, which adopts the principle of superposition and which was taken to figure out the pressure decline over time at the reservoir top, can be used to calculate the current pressure at various depths of the reservoir.

The results of the calculations, represented in graphic form in Fig. 9, show that the pressure drop is negligible for $X_D^* \approx 2$. This allows us to affirm that the depressurization of the reservoir is limited to a depth of 3h. Being h probably a few hundred meters, it follows that depressurization should not have involved the part of the reservoir at depths over 2000 m.

6. CONCLUSIONS

The model described in this paper has been successfully used to calculate the reservoir pressure drop in the Valle Secolo area of the Larderello field, caused by the field exploitation. The fitting of the field data by the model's results has also allowed us to estimate the hydraulic diffusivity η, the fluid compressibility Φc and the vertical pressure distribution in the reservoir. Such a distribution has been calculated after 30 years of exploitation and therefore is that should exist at present.

It shows that the depressurization of the reservoir turns out to be restricted to a depth of some 2000 m. Recent results obtained by deepening old wells (S. Martino 2, Campo ai Peri, VC8, 156, 119) reveal indeed the existence of a vertical pressure gradient in the reservoir much higher than that due to static steam, consequently reveal a substantial pressure increase with depth in agreement with the model.

The calculations have been restricted to the Valle Secolo area, but it has been verified however that the shut-in wells in the Gabbro area, area exploited some ten years after the Valle Secolo, possess a pressure history qualitatively similar to that foreseen by the model.

This observation shows also that the drainage on the Gabbro area, due to the Valle Secolo wells, is rather weak.

If this low interference (in a horizontal direction) is generalizable for the different producing areas of the whole geothermal field, then we can think that significant reserves of fluid might well still be located at modest depths in the areas where density of production is low.

This consideration seems to be actually confirmed by the drilling of new wells in areas of the Larderello field which are weakly exploited (Val di Cornia, Monteverdi).

ACKNOWLEDGEMENTS

I wish to thank G.Allegrini, who promoted and encouraged this work and A.Barelli for useful suggestions in writing of this paper.

REFERENCES

[1] NERI G. Flow Rate Decline and Pressure Transients in the Larderello Geothermal Field.Proc.13th Workshop on Geothermal Reservoir Engineering.Stanford 1987.

[2] CARSLAW H.S., JAEGER J.C. - Conduction of Heat in Solids - Oxford University Press,2nd Ed.,p.306, London 1959.

[3] WHITE D.E.,MUFFLER L.J.P. and TRUESDELL A.H.-Vapor dominated Hydrotermal Systems Compared with Hot Water Systems.Econ.Geol. 66,1971.

[4] GRANT M.A.,DONALDSON I.A.,BIXLEY P.F. Geothermal Reservoir Engineering.Academic Press 1982.

KEY TO SYMBOLS

P Pressure
G Mass flow-rate
Q Flow-rate in volume
V Volume
A Surface area of flow
R^- = R/Mw where R is the perfect gases constant and Mw is the molecular weight of water
K Permeability
μ Dynamic viscosity
z Compressibility factor for steam
η Diffusivity
Φ Porosity
c Fluid compressibility
r Density
x Position coordinate
t Time

Grad Gradient operator
erf Error function
erfc Complementary error function
e or exp Exponential function

Subscripts

$_{1,2}$ Region indices
$_{i}$ Time index
$_{21}$ Used in Q_{12} to indicate flow from Region 2 to Region 1
$_{D}$ Indicates a dimensionless entity

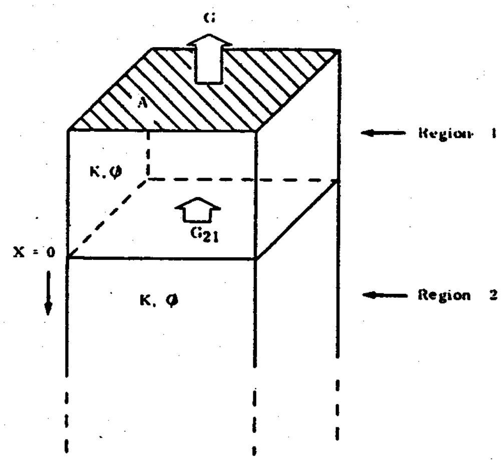

FIG. 1
- Scheme of the reservoir as used for the formulation of the mathematical model.

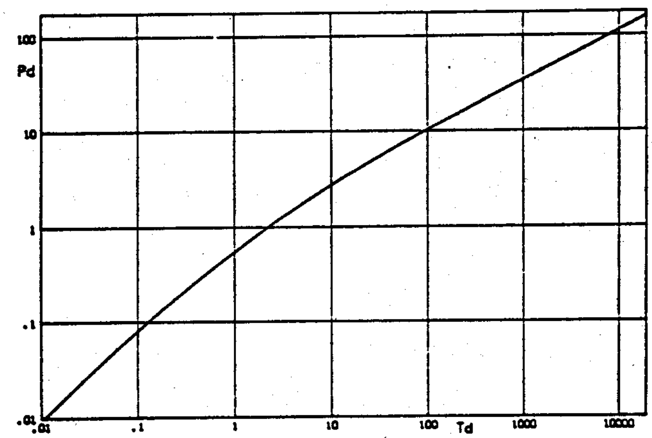

FIG. 2
- Graph of the influence function P_D^* as a function of t_D^*

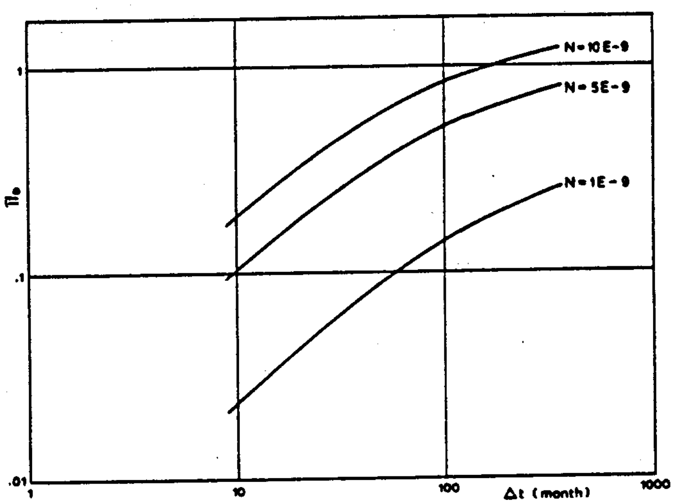

FIG. 3
- Graph of the dimensionless pressure π_D as a function of time and for various values of the parameter $N^{\sim}$.

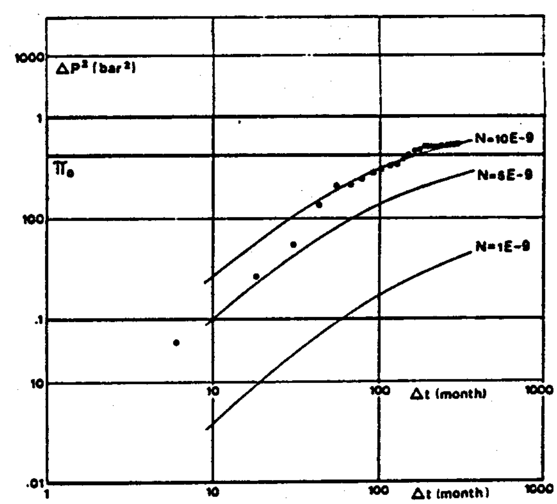

FIG . 4
- Graph of δ $(P^*) = P_1^* - P^*(t)$ of well 111 in Larderello, as a function of time, interpolated with the function calculated with the mathematical model.

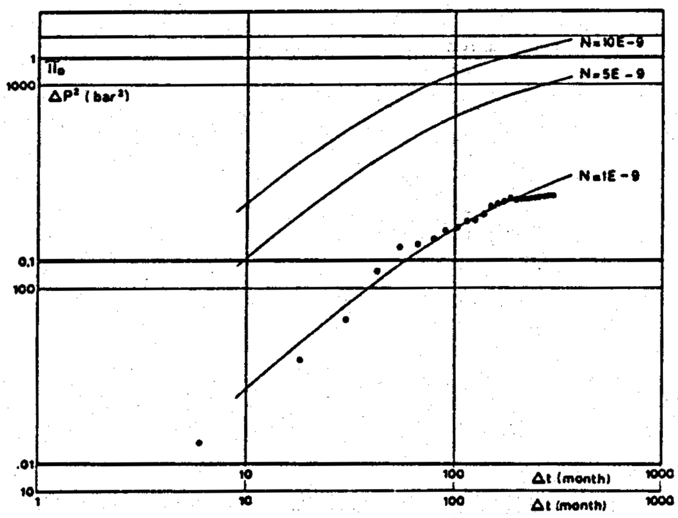

FIG. 5
- Graph of $\delta\ (P^2) = P_1^2 - P^2(t)$ of well 111 in Larderello, as a function of time, interpolated with the function calculated with the mathematical model.

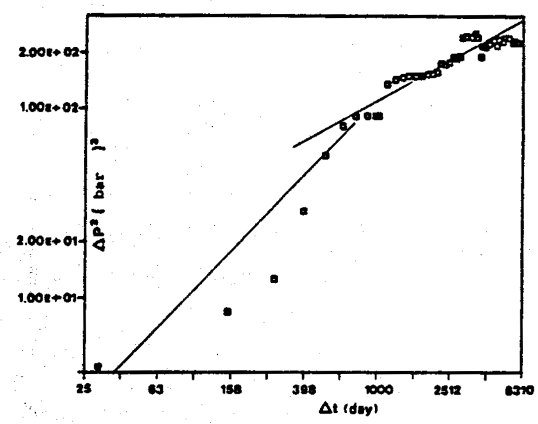

FIG. 7
Graph of $\delta(P^2) = P_1^2 - P^2(t)$ of well Gabbro 8 as a function of time.

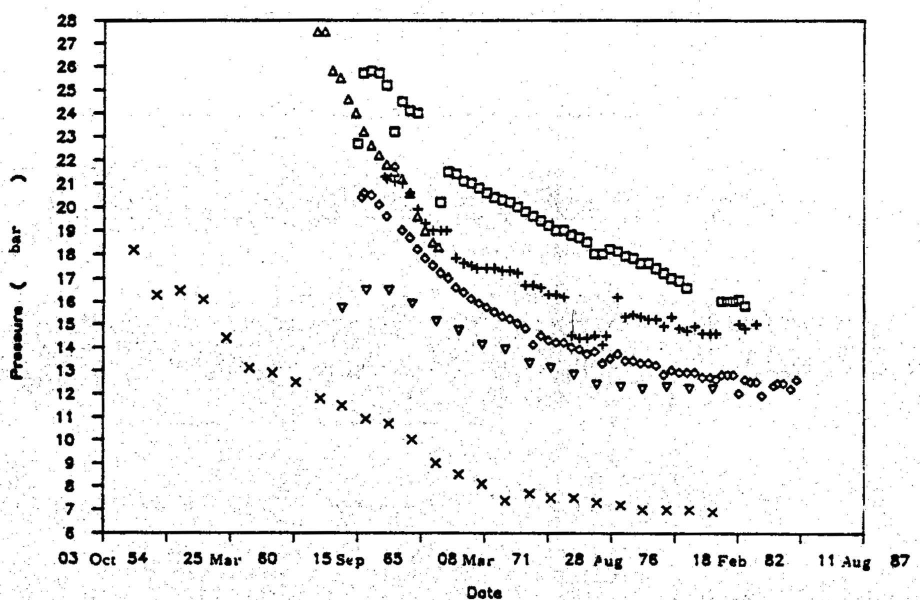

FIG. 6
- Pressure decline of some closed wells in the Valle Secolo and Gabbro areas.

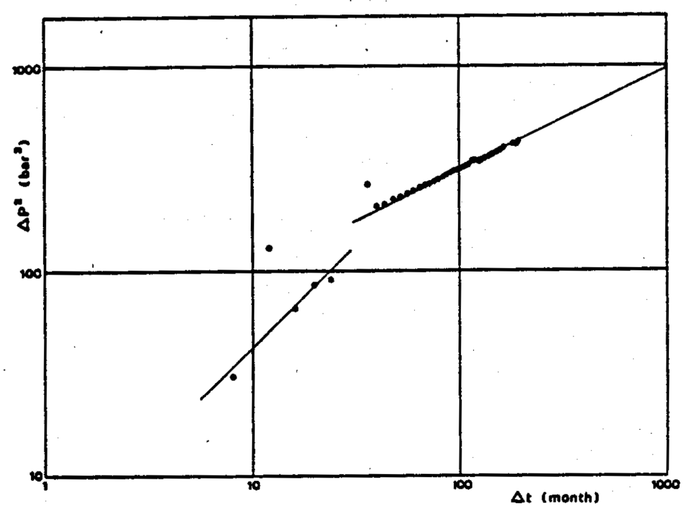

FIG. 8
- Bilogarithmic graph of $\delta(P^2) = P_1^2 - P^2(t)$ of well S. Dalmazio 4 as a function of time.

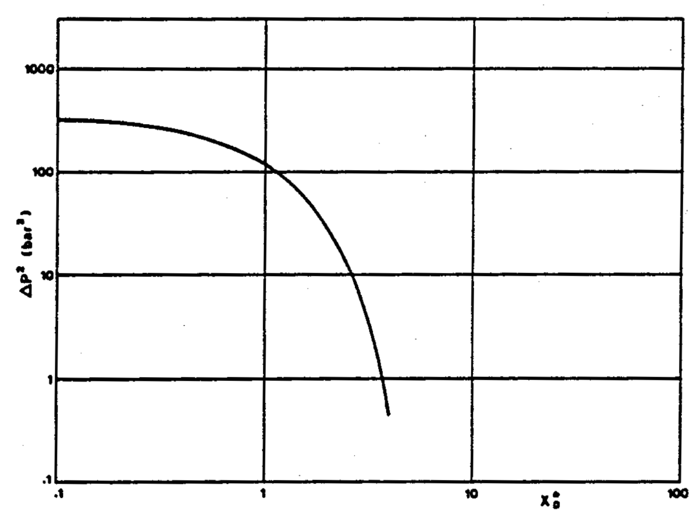

FIG. 9
- Graph of $\delta(P^2) = P_1^2 - P^2(t)$ as a function of dimensionless depth X_D^*, calculated with the mathematical model for $N^- = 10^{-9}\ s^{-1}$ and $t = 360$ months.